



# Effects of short-term endurance and strength exercise in the molecular regulation of skeletal muscle in hyperinsulinemic and hyperglycemic *Slc2a4*<sup>+/-</sup> mice

Vitor Rosetto Muñoz<sup>1</sup> · José Diego Botezelli<sup>1</sup> · Rafael Calais Gaspar<sup>1</sup> · Alisson L. da Rocha<sup>1</sup> · Renan Fudoli Lins Vieira<sup>1</sup> · Barbara Moreira Crisol<sup>1</sup> · Renata Rosseto Braga<sup>1</sup> · Matheus Brandemarte Severino<sup>2</sup> · Susana Castelo Branco Ramos Nakandakari<sup>3</sup> · Gabriel Calheiros Antunes<sup>1</sup> · Sérgio Q. Brunetto<sup>4</sup> · Celso D. Ramos<sup>4,5</sup> · Lício Augusto Velloso<sup>6,7</sup> · Fernando Moreira Simabuco<sup>2</sup> · Leandro Pereira de Moura<sup>1,6</sup> · Adelino Sanchez Ramos da Silva<sup>8</sup> · Eduardo Rochete Ropelle<sup>1,6,9</sup> · Dennys Esper Cintra<sup>3,6</sup> · José Rodrigo Pauli<sup>1,6,9</sup>

Received: 5 November 2022 / Revised: 8 March 2023 / Accepted: 28 March 2023 / Published online: 13 April 2023  
© The Author(s), under exclusive licence to Springer Nature Switzerland AG 2023

## Abstract

**Objective** Intriguingly, hyperinsulinemia, and hyperglycemia can predispose insulin resistance, obesity, and type 2 diabetes, leading to metabolic disturbances. Conversely, physical exercise stimulates skeletal muscle glucose uptake, improving whole-body glucose homeostasis. Therefore, we investigated the impact of short-term physical activity in a mouse model (*Slc2a4*<sup>+/-</sup>) that spontaneously develops hyperinsulinemia and hyperglycemia even when fed on a chow diet.

**Methods** *Slc2a4*<sup>+/-</sup> mice were used, that performed 5 days of endurance or strength exercise training. Further analysis included physiological tests (GTT and ITT), skeletal muscle glucose uptake, skeletal muscle RNA-sequencing, mitochondrial function, and experiments with C2C12 cell line.

**Results** When *Slc2a4*<sup>+/-</sup> mice were submitted to the endurance or strength training protocol, improvements were observed in the skeletal muscle glucose uptake and glucose metabolism, associated with broad transcriptomic modulation, that was, in part, related to mitochondrial adaptations. The endurance training, but not the strength protocol, was effective in improving skeletal muscle mitochondrial activity and unfolded protein response markers (UPRmt). Moreover, experiments with C2C12 cells indicated that insulin or glucose levels could contribute to these mitochondrial adaptations in skeletal muscle.

**Conclusions** Both short-term exercise protocols were efficient in whole-body glucose homeostasis and insulin resistance. While endurance exercise plays an important role in transcriptome and mitochondrial activity, strength exercise mostly affects post-translational mechanisms and protein synthesis in skeletal muscle. Thus, the performance of both types of physical exercise proved to be a very effective way to mitigate the impacts of hyperglycemia and hyperinsulinemia in the *Slc2a4*<sup>+/-</sup> mouse model.

**Keywords** Physical exercise · Hyperinsulinemia · Mitochondrial adaptations · Skeletal muscle

## Introduction

Hyperinsulinemia may precede body fat gain, insulin resistance, and type 2 diabetes (T2D) development [1–3]. The molecular mechanisms connecting hyperinsulinemia to metabolic diseases and body fat gain have not yet been fully elucidated. Moreover, defects in skeletal muscle insulin signaling are observed much earlier than the onset of T2D in people with genetic risk [4]. In humans, skeletal muscle is the primary tissue involved in peripheral insulin resistance, contributing to insulin secretion by  $\beta$ -cells, insulin circulating levels, insulin resistance, and inflammation, factors

Vitor Rosetto Muñoz and José Diego Botezelli have contributed equally to this work.

✉ Vitor Rosetto Muñoz  
vitor.munoz93@gmail.com

✉ José Rodrigo Pauli  
rodrigopaulifca@gmail.com

Extended author information available on the last page of the article

related to cardiometabolic risk [5, 6]. Prolonged insulin treatment may reduce insulin responsiveness in humans, corroborating that hyperinsulinemia can cause insulin resistance [7, 8]. Conversely, in experimental models, reduced insulin levels are accompanied by decreased cardiometabolic risk and an extended lifespan [9–11].

The regulation of cellular glucose uptake is tightly controlled by several upstream factors that sense and respond to fluctuations in systemic glucose levels, maintaining blood glucose within a narrow window of normality [12]. Glucose uptake is mediated by different glucose transporters that are present in distinct metabolic tissues. The Glucose Transporter type 4 (GLUT4), encoded by the Solute Carrier Family 2 Member 4 (*Slc2a4*) gene, plays a pivotal role in skeletal muscle, adipose tissue, and brain glucose uptake [12, 13]. Some stimuli, such as physical exercise or eating positively affect the translocation of GLUT4 to the cell membrane, facilitating glucose uptake to the intracellular compartment, and thus, reducing blood glucose levels [14]. However, metabolic disarrangements are associated with poor regulation of glucose uptake and a chronic hyperglycemic/hyperinsulinemic state [14]. In addition, mitochondrial dysfunction and insulin signaling abnormalities are implicated in the pathogenesis of insulin resistance, the hallmark of T2D [15, 16]. A compilation of recent studies suggests that upregulation and enhancement of mitochondrial function may represent a valuable therapeutic strategy to improve insulin sensitivity [15].

Herein, we proposed to study the initial responses to endurance and strength physical exercise in the heterozygous *Slc2a4* mouse line (*Slc2a4*<sup>+/-</sup>), that harbors GLUT4 content, accompanied by hyperglycemia, hyperinsulinemia, insulin resistance, and glucose intolerance, but without the presence of increased body adiposity. Although this is a previously characterized model [17], our objective was to explore two short-term exercise protocols (aerobic and strength) that did not generate changes in weight and body fat to assess transcriptional and translational adaptations in skeletal muscle. It should be noted that the vast majority of studies that have explored the impacts of physical exercise on glucose metabolism have done so in models of diet-induced or genetically modified obesity in which animals show increased adiposity [18, 19]. Another strategy used to induce hyperglycemia and hyperinsulinemia is the administration of glucocorticoids, which is also associated with changes such as loss of muscle mass and an increase in abdominal fat [20]. Other studies that investigated the effects of exercise on skeletal muscle metabolism were conducted with lean animals and, therefore, without changes in circulating insulin and glucose levels.

Both aerobic and strength exercise have pleiotropic effects on nearly all organ systems, likely with some overlapping mechanisms [21]. Therefore, our challenge here was to study

the effects of short-term physical exercise on the variables hyperglycemia and hyperinsulinemia and, with this, demonstrate how exercise protocols can attenuate this pathophysiological condition. Moreover, the findings will contribute to the understanding of the impacts of aerobic and strength exercise on conditions of hyperglycemia and hyperinsulinemia, which are manifestations that may precede the development of obesity and T2D, with both types of exercise having specific responses that contribute to glycemic homeostasis at the beginning of a physical training program.

## Methods

### Experimental animals

Male *Slc2a4*<sup>+/-</sup> mice (heterozygous) were obtained by crossing *Slc2a4*<sup>-/-</sup> females (homozygous) with *Wild-Type* males purchased from Cyagen®. The generation of this model was performed by a pair of TALENs targeting exon 4 of the *mSlc2a4* gene (NM\_009204.2). The DNA from the tail was extracted, amplified, and sequenced to confirm the genotype of each animal. The following primer was utilized: mSlc2a4-R: 5'-GCCGAGGATAGCTGCATATTCCA-3; with 466 bp product size and 59 °C annealing temperature. All the experiments were conducted according to the Ethics Committee of UNICAMP (5107-1/2018 and 5003-1/2018), and the animals were conditioned to their cages (n = 5/cage) at 22 °C with free access to water and a standard diet (Nuvilab). The experimental groups were distributed into (1) *Wild-Type* (WT): 8-month-old sedentary mice; (2) Sedentary *Slc2a4*<sup>+/-</sup>: 8-month-old sedentary *Slc2a4*<sup>+/-</sup> mice; (3) Endurance exercised *Slc2a4*<sup>+/-</sup>: 8-month-old *Slc2a4*<sup>+/-</sup> mice that performed the endurance exercise training protocol; and (4) Strength exercised *Slc2a4*<sup>+/-</sup>: 8-month-old *Slc2a4*<sup>+/-</sup> mice that performed the strength exercise training protocol. At least n = 7 mice/group were utilized from different cohorts. Some of the animals were intraperitoneally injected with Puromycin (40 nM/g of body weight in 1 × PBS, # P-600–100, Gold Biotechnology®) and the gastrocnemius collected after 20 min. These mice have an important particularity and partial deficiency of GLUT4 in the body, becoming hyperglycemic and hyperinsulinemic, with no change in body adiposity, and thus allowing the assessment of the effects of aerobic and resistance physical exercise in a unique way in the face of this metabolic challenge.

### Short-term endurance exercise training protocol

Before performing the endurance exercise training protocol, *Slc2a4*<sup>+/-</sup> mice were adapted to the treadmill for 5 days at 10 m/min for 10 min (AVS Projetos®, São Carlos, Brazil). After this period, the incremental load test (ILT) was

performed, beginning with the intensity of 3 m/min with 3 m/min increments every 3 min until identification of the exhaustion velocity of each animal. This exhaustion velocity was used to prescribe the endurance exercise protocol intensity. After a 48 h washout, the mice performed 5 days of endurance exercise training (60 min running at 60% of exhaustion velocity) followed by a 16 h rest period to perform the glucose tolerance test (GTT). On the next day, the mice were submitted to another session of endurance exercise training followed by performance of the insulin tolerance test (ITT) 16 h after the last exercise session. Another session was conducted on the next day, and the tissue collection was performed 16 h after the last exercise training session. The endurance exercise protocol was carried out over a total of 7 days.

### Short-term strength exercise training protocol

Prior to the strength exercise training protocol, the mice were adapted to a climbing ladder (AVS Projetos<sup>®</sup>, São Carlos, Brazil). The ladder used was 70 cm high, 10 cm wide, with 1.5 cm between steps, an 80° inclination, and a 30 cm<sup>2</sup> dark chamber at the top of the ladder. The adaptation was conducted for 5 days by placing the animals in the dark chamber (1 min) before climbing. Subsequently, the animals were positioned 15, 25, and 70 cm below the dark chamber in three different attempts to conclude 1 day of adaptation. A canonical plastic tube was attached with adhesive tape to the animals' tails with no load during the adaptation. An incremental load test on the climbing ladder was performed to determine the maximal voluntary carrying capacity (MVCC). This test began with 75% of body weight attached to the tail, followed by 5 g increments in each climb. The climb was considered successful when the animal climbed 70 cm (that represents ~ 12 dynamic movements with each leg). A 5 min rest period was used between each attempt. When the animals could not complete the climb, the previous carrying capacity was used to prescribe the individual load for each animal.

After determining the MVCC, a 48 h period washout was applied, and the strength exercise training protocol was started. Each exercise session consisted of 20 climbs (~ 30 s/climbing) with 70% of the MVCC load and 60 s intervals between each climb. Each exercise session per animal has a duration of 10–15 min of climbing and 19 min of rest between the climbs, totalizing ~ 30 min of training for each animal. Firstly, the animals performed 5 days of strength exercise training followed by a 16 h rest period to complete the GTT. On the next day, the mice were submitted to another session of strength exercise training followed by a 16 h rest to perform the ITT. Another session was conducted on the next day before the tissue collection 16 h after the last

exercise training session. The strength exercise protocol was carried out over a total of 7 days.

### Behaviour and performance tests

To evaluate any stress effect from exercise protocols, the exercised mice were submitted to Elevated Plus Maze (EPM) and Open Field (OF) tests as described previously [22, 23]. The EPM apparatus was composed of two open arms (25 × 5 × 0.5 cm), perpendicularly crossed with the closed arms (25 × 5 × 16 cm), and 50 cm above the floor. The OF was performed in a circular wooden ring (81 cm diameter) with 41 cm walls. Approximately 30 min prior to the EPM and OF tests, the mice were transferred to the test room. Each mouse was placed in the center of the apparatus and they were recorded for 10 min for further analysis.

In another cohort of animals, the *Slc2a4*<sup>+/-</sup> mice, the animals performed the grip strength test on the 1st day. After that, on the 2nd day, they initiated the treadmill or the climbing ladder adaptation (4 days). On the 5th day, both groups performed the exhaustion velocity test. After a 24 h washout (7th day), mice were submitted to the MVCC, followed by another 24 h washout. These tests were considered the pretreatment performance. On the 8th day, the *Slc2a4*<sup>+/-</sup> mice were submitted to 7 days of a short-term endurance or strength exercise training protocol as described previously. Twenty-four hours after the final exercise session (15th day), mice from both groups performed the grip strength test in the morning and the exhaustion velocity test in the afternoon. On the 16th day and 48 h after the last exercise session, the mice performed the MVCC test. These results were considered the posttreatment performance.

### Metabolic parameters (ITT and GTT) and serum analysis

The GTT was performed after 5 days of the endurance or strength exercise training protocol and 16 h after the final exercise session (with a 6 h fasting period). Tail blood was collected to measure the fasting glycemia (0' of the GTT) using a glucometer (Accu-Chek glucometer, Roche Diagnostics<sup>®</sup>), and a 25% glucose solution was injected intraperitoneally (i.p.) at 2 g/kg to measure the glycemia after 30, 60, and 120 min.

After another exercise training period (6 days of exercise), the ITT was performed. Under the same conditions (16 h after the final exercise session and with a 6 h fasting period), tail blood was used to obtain the fasting glycemia (0' of the ITT), and an i.p. injection of 0.3% insulin (1.5 U/kg, Humulin R; Lilly<sup>®</sup>, Indianapolis, IN, USA) was administered. The glycemia was monitored for 5, 10, 15, 20, 25, and 30 min after the insulin injection.

On the day of the tissue collection (after 7 days of exercise, 16 h after the final exercise session, and with a 6 h fasting period), before the anesthesia injection, the blood from the tail was collected to measure the fasting glycemia, centrifuged (3000 rpm, 4 °C, for 5 min) to collect the serum, and stored at – 80 °C for future analysis. In another cohort of *Slc2a4*<sup>+/-</sup> animals, the serum was collected before the beginning of the exercise protocol and after 16 h and 90 h. The insulin in the serum was measured using an enzyme-linked immunosorbent assay (RayBiotech®, Norcross, GA; #ELM-Insulin). The calculation: [fasting plasma glucose (mmol/L) × fasting plasma insulin (μU/mL)/22.5] was used to determine the Homeostatic Model Assessment of Insulin Resistance (HOMA-IR) index with the glycemic and insulin levels obtained from the exact moment of collection. The serum biochemical parameters (TG, cholesterol, and HDL) were determined using commercial colorimetric kits (Laborlab®, São Paulo, Brazil). The corticosterone levels were measured using Luminex TM multiplex reagents (MSHMAG-21 k-05, Merck Millipore®) following the instructions in the Luminex 200 instrument with xPONENT 3.1

### Molecular analysis (immunoblotting and RT-qPCR)

At the end of the experiment and 16 h after the final exercise session, the animals fasted for 6 h and were anesthetized (90 mg/kg ketamine chloral hydrate and 10 mg/kg xylazine). The tissues were then collected and stored in liquid nitrogen at –80 °C. Some of the animals were insulin-stimulated with 7 U/kg insulin intraperitoneal injection 10 min before the tissue extraction. The samples used in the immunoblotting were homogenized in a protein extraction buffer (1% Triton-X 100, 100 mM Tris (pH 7.4), 100 mM sodium pyrophosphate, 100 mM sodium fluoride, 10 mM EDTA, 10 mM sodium vanadate, 2 mM PMSF, and 0.1 mg of aprotinin/ml) using TissueLyser II (Qiagen®), followed by centrifugation (12000 rpm, 4 °C for 15 min) and the supernatant was collected. In the case of pgWAT, ingWAT, and BAT, the centrifugation was performed twice. The protein concentration was measured using the bicinchoninic acid method. The samples were prepared using ~ 30 μg of protein and Laemmli 6x, then submitted to SDS-PAGE. The gels with the samples were transferred to a nitrocellulose membrane, blocked with 5% mil (50 min, RT), washed (TBS + Tween), and incubated (4 °C overnight) with the following primary antibodies: Puromycin #MABE343, pTBC1D1 (S237) #072268 from Millipore®; pIRβ (Y972) #GTX25678 from GeneTex®; GLUT4 (*Slc2a4*) #2213, GLUT1 (*Slc2a1*) #12939, pIGF1Rβ (Y1131) #3021, IGF1Rβ #9750, IRβ #3025, pAkt (Thr308) #13038, pAkt (S473) #4060, Akt #4685, pAS160 (Thr642) #4288, pERK1/2 (T202/Y204) #4370, pTSC2 (Thr1462) #3611, pmTOR (S2448) #2971, mTOR #2983, pEIF2α (S51) #9721, EIF2α #9722, pS6K (Thr389) #9234, S6K

#2708, Tfam #8076, VDAC #4866, OPA1 #80471, β-actin #370, GAPDH #2118, Vinculin #4650, α-tubulin #2144 from Cell Signaling Technology®; pIRS1 (Y612) #sc-17195, IRS1 #sc-559, CLPP #ab124822, from Santa Cruz Biotechnology®; Nrf1 #ab55774, OXPHOS #ab110413 from ABCAM®, HSP60 #bs-0191R, LONP1 #bs-4245R from Bioss®, and YME1L1 #11510-AP, PINK1 #23274–1-AP from Proteintech®. After the primary antibody incubation, a secondary antibody (rabbit or mouse) was used. The membranes were washed and incubated for 50 min at RT and labeled with chemiluminescence reagent (ECL), followed by image acquisition with G:Box XR5 (Syngene®, Frederick, MD, USA). The densitometry of the band was measured using UN-SCAN-IT gel 6.1® software.

The real-time polymerase chain reaction (RT-qPCR) analysis was performed using complementary DNA (cDNA) obtained from a small fragment of tissue (~ 30 mg) that was lysed in Trizol (Life Technologies®, USA) and submitted to the RNA extraction protocol. The cDNA was synthesized (2 μg) with High-Capacity cDNA Reverse Transcription Kits (Applied Biosystems®, Forest City, CA) and subjected to RT-qPCR in a reaction composed of 100 ng cDNA, 150 nM primers (reverse and forward), and 2 × iTaq Universal SYBR Green Supermix (Bio-Rad®, Hercules, CA, USA) in the 7500 Fast Real-Time PCR System (Applied Biosystems®, Forest City, CA). The Ct values were adopted to obtain the ΔΔCt of target genes normalized by a housekeeping gene (*Actb*). The primer sequences are described in Table S1.

### [<sup>18</sup>F]-FDG uptake in skeletal muscle

Skeletal muscle glucose uptake was determined using a small animal Positron Emission Tomography and Computed Tomography (PET/CT) in vivo imaging system (Albira, Bruker®, Massachusetts, USA). The images were analyzed using the PMOD workstation. The animals were anesthetized with 2% isoflurane and 5 MBq of 2-deoxy-2-[<sup>18</sup>F]-fluoro-d-glucose ([<sup>18</sup>F]-FDG, obtained from Nuclear and Energy Research Institute-IPEN, Sao Paulo, Brazil) was injected in the retro-orbital sinus. The CT was performed with 80 kVp, 160 μA, and 1024 projections, during 0.8 s per CT rotation, pitch 4.0–5.0 mm, a field of view of 71.3 mm, and a scan speed of 24.6 mm/s. After the CT scan, the PET scan was initiated, keeping the animal in the same position in the craniocaudal direction. The PET scan was started 60 min after [<sup>18</sup>F]-FDG injection and lasted 40 min. The scans were reconstructed using PMOD in the LabPET software, calibrating the images in Bq/mL from a scanned phantom cylinder. The region of interest (ROI) was constructed using CT scans to access the three-dimensional uptake volume in the gastrocnemius muscle. The images were converted to standardized uptake values (SUVs), normalized by the animal's body weight. The PET scans were performed

without or with insulin (0.5 U/Kg, i.p. injection) in an  $n = 3$ /group per condition.

### RNA-sequencing

Total RNA was isolated from gastrocnemius muscle with the Trizol (Life Technologies<sup>®</sup>, USA) and chloroform/isopropanol/ethanol method and sequenced by BRC Sequencing Core at the University of British Columbia. The RNA quality was checked in an Agilent 2100 Bioanalyzer instrument. After the quality test, the library was prepared using a Stranded polyA + mRNA kit (Illumina TruSeq mRNA stranded). The samples were then sequenced on the Illumina NextSeq 500 with Paired-End 42 bp  $\times$  42 bp reads. The sequences were aligned to the *Mus Musculus mm10* sequence with a STAR aligner. The raw counts were normalized. Differential expression between groups was performed using the DESeq2 package, and Benjamini & Hochberg adjusted to a  $p$  value  $< 0.05$  cut-off. The gene ontology analysis (biological process, cellular components, and molecular functions) was performed using DAVID platform V6.8. The fasting glucose and insulin levels of each mouse were correlated with the normalized raw count of each gene ( $R =$  Spearman coefficient). The heatmaps were built using Gene-E online software (<https://software.broadinstitute.org/GENE-E/>).

### Histological analysis and immunofluorescence

During tissue extraction, small fragments collected from gastrocnemius, liver, perigonadal white adipose tissue (pgWAT), inguinal (ingWAT), and brown adipose tissue (BAT) were fixed in 4% PFA for 24 h. The tissue was dehydrated, embedded in paraffin, and sliced at 10  $\mu$ m in a microtome (Leica<sup>®</sup>, RM2145). The slides were hydrated again and stained with hematoxylin–eosin (H&E) solution. The H&E images were acquired in optical microscopy (LAB2000, LABORANA<sup>®</sup>, São Paulo, Brazil) with MotiCam Pro 282B 5.0 megapixels (Motic<sup>®</sup>, Hong Kong, China). The slides of gastrocnemius samples were immunostained with GLUT4 primary antibody (NBP-49533) from Novus Biologicals<sup>®</sup>, followed by goat anti-rabbit rhodamine (sc-2091, from Santa Cruz Biotechnology<sup>®</sup>) secondary antibody incubation. The primary antibody was diluted at 1:100 in 1.5% BSA and the secondary antibody at 1:200 in 1.5% BSA. The nucleus was stained with DAPI (#H-1200; Vector Laboratories, Burlingame, CA, USA). The slides were coverslipped and the images were acquired using Leica Application Suite software (at 20  $\times$  magnification). Positive staining was considered as the mean of five muscle sections of each group using CorelDraw 2019 software.

### High-resolution respirometry (mitochondrial function)

The oxygen consumption of skeletal muscle (50 mg of gastrocnemius) and C2C12 cell ( $1.5 \times 10^6$ ) samples was measured using Oxygraph-2 k (Oroboros Instruments<sup>®</sup>, Innsbruck, Austria). Sixteen hours after the final exercise session, 50 mg of gastrocnemius sample was submitted to muscle fiber dissociation using forceps and permeabilized with 50  $\mu$ g/mL saponin (under agitation, 30 min, at 4  $^{\circ}$ C). The muscle fibers were then transferred to the equipment chambers in 2 mL of mitochondrial respiration medium (MIR). The C2C12 cells were cultured in 100 mm dishes and treated for 24 h, followed by trypsinization and resuspension in 2 mL of MIR. The samples were placed in the equipment chambers. The basal respiration was obtained (with 0.5 mM malate, 10 mM glutamate, and 5 mM pyruvate), then 2.5 mM ADP were added to measure complex-I-dependent respiration. Next, 10 mM succinate was injected (Complex I and II respiration), with 2.5 mM oligomycin (ATP synthase inhibitor), to measure the mitochondrial coupling, and 0.5 mM FCCP, to measure the mitochondrial uncoupling.

### Cell culture

In the cell culture experiments, C2C12 cells (ATCC<sup>®</sup> CRL-1772<sup>TM</sup>) were grown in Dulbecco's Modified Eagle's Medium (DMEM, #12100046, ThermoFisher scientific<sup>®</sup>) with 10% of fetal bovine serum (FBS—Gibco<sup>®</sup> #A476680), and 1% of Penicillin/Streptomycin complexes (P/S—Gibco<sup>®</sup> #15140122) at 37  $^{\circ}$ C, 5% CO<sub>2</sub>, and  $\sim 80\%$  of confluence. To perform the mitochondrial respiration experiments, the C2C12 cells were cultured in 100 mm cell culture dishes in a low glucose medium (1000 mg/L #11885084, ThermoFisher scientific<sup>®</sup>), high glucose medium (4500 mg/L, #12100046, ThermoFisher scientific<sup>®</sup>), or a DMEM containing insulin (50 nM, 24 h). The cells were trypsinized, and  $1.5 \times 10^6$  cells were resuspended in 2 mL MIR to evaluate the mitochondrial respiration. A portion of these cells were plated in a 6-well plate ( $1.5 \times 10^5$ ) and treated for 24 h in the same conditions to collect the protein lysate. The C2C12 cells were treated with tetracycline (30  $\mu$ g/mL, 24 h) after plating in a 6-well plate. In another set of experiments, these tetracycline-treated cells were stimulated or not with insulin (20 nM, 15 min) and collected for immunoblotting analysis. Intracellular glucose uptake was performed by adding 2-NBDG (#N13195, Invitrogen<sup>®</sup>) and insulin (100 nM) for 30 and 60 min to the cells as described previously [24]. For protein synthesis measurement, cells were exposed to puromycin (1  $\mu$ M) for 30 min and collected for immunoblotting analysis.

## Oxygen consumption, respiratory exchange ratio (RER), and heat production

In another cohort, the animals were submitted to 5 days of the exercise training protocol. They were acclimated in individual cages of the Comprehensive Lab Animal Monitoring System (CLAMS, Oxymax, Columbus Instruments®) for 24 h. The oxygen consumption (VO<sub>2</sub>), carbon dioxide consumption (VCO<sub>2</sub>), respiratory exchange ratio (RER), and heat production (Heat) were recorded over a 24 h period after the 1st day of adaptation. The data were analyzed and separated for the animals according to the dark and light cycle, using a n = 5/group.

### Statistical analysis

The data were analyzed by the Student *t*-test to compare differences between two groups or ONE-way Analysis of Variance (ANOVA) followed by Tukey's post hoc test to compare more than two groups. In the time-dependent analysis (GTT and ITT), a two-way ANOVA test followed by Tukey's was used with a simple effect within rows. The graphs were built in GraphPad Prism 8.0.1® software, expressing the data

as mean ± standard error of the mean (SEM). The statistical significance adopted was *p* < 0.05.

## Results

### Endurance and strength exercise improves whole-body insulin sensitivity and glucose tolerance in *Slc2a4*<sup>+/-</sup> mice

First, our model was validated by DNA sequencing and *Slc2a4* protein content quantification (Fig. 1A, B). The hyperglycemic and hyperinsulinemic phenotypes were also validated following these parameters over the months (data not shown), which were similar to those previously observed [17]. The *Slc2a4*<sup>+/-</sup> mice showed increased fasting glucose, fasting insulin, and HOMA-IR, but this was reversed by endurance or strength short-term exercise training (Fig. 1C–E). In addition, the effects of endurance and strength exercise on *Slc2a4*<sup>+/-</sup> mice related to the fasting glucose and insulin levels were lost 90 h after the final exercise session (Fig. S1A–B). The *Slc2a4*<sup>+/-</sup> also presented insulin resistance and glucose intolerance, which were

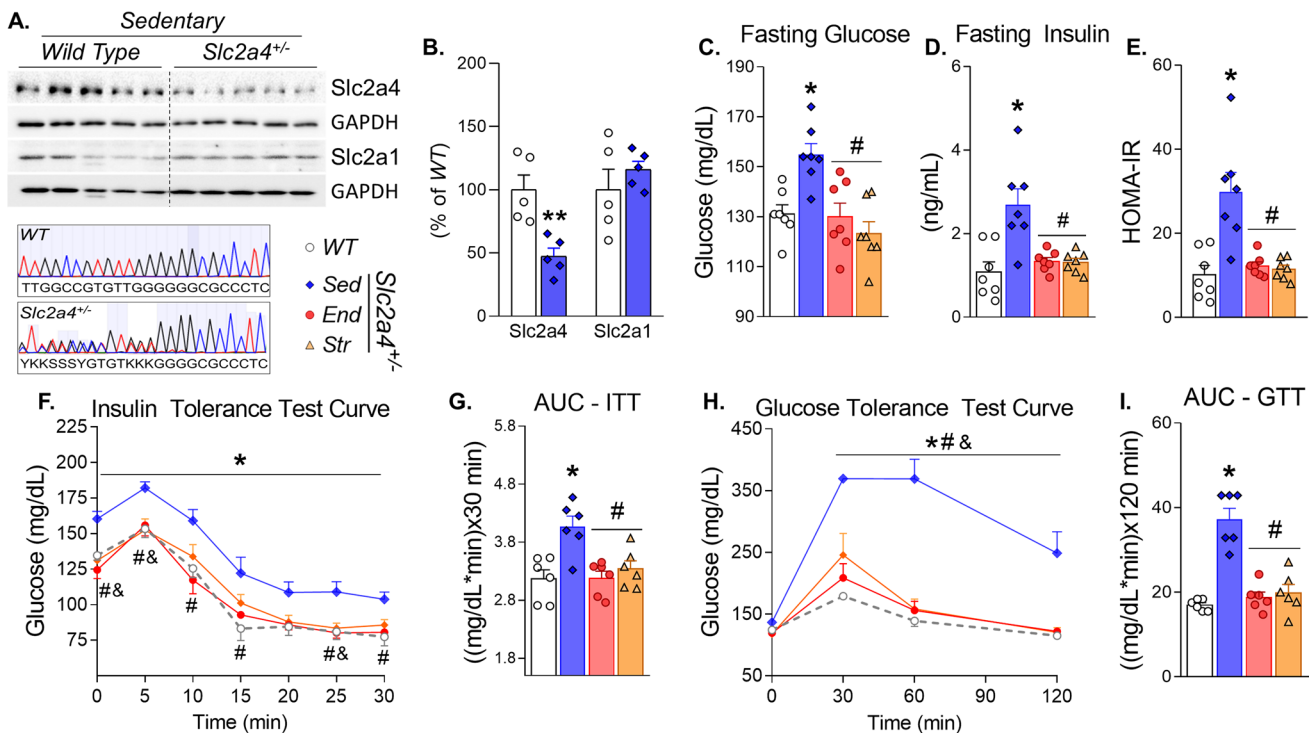


**Fig. 1** Physiological parameters. **A** Genotyping and validation of Wild Type (WT) and *Slc2a4*<sup>+/-</sup> mice. **B** SLC2a4 and SLC2a1 protein content in the gastrocnemius muscle (n = 5/group). **C** Fasting glucose. **D** Fasting Insulin. **E** HOMA-IR index. **F** Insulin tolerance test (ITT) curve. **G** Area under the curve (AUC) of the ITT. **H** Glucose tolerance test (GTT) curve. **I** Area under the curve (AUC) of the GTT. In

**C–E**, n = 7/group was used. In **F–I**, n = 6/group was used. \**p* < 0.05 vs WT group. #*p* < 0.05 vs *Slc2a4*<sup>+/-</sup> Sedentary group. In the graphs **F** and **H**, \**p* < 0.05 WT vs *Slc2a4*<sup>+/-</sup> Sedentary, #*p* < 0.05 *Slc2a4*<sup>+/-</sup> Sedentary vs *Slc2a4*<sup>+/-</sup> Endurance, &*p* < 0.05 *Slc2a4*<sup>+/-</sup> Sedentary vs *Slc2a4*<sup>+/-</sup> Strength

counteracted by both exercise training protocols (Fig. 1F–I). These results were observed without significant changes in the body weight, Lee index, and adipose tissue weight (Fig. S1C–F). There was greater liver weight in the *Slc2a4*<sup>+/-</sup> sedentary mice, which was attenuated by endurance exercise training (Fig. S1H). Moreover, no significant changes were observed in the serum biochemical parameters (TG, Cholesterol, HDL), hepatic gluconeogenic enzyme expression (*Pepck*, *G6pase*, and *Pc*), and hepatic morphological aspects (Fig. S1G, I, J).

### Insulin signaling and transcriptomic analysis in skeletal muscle

The physiological changes observed in the *Slc2a4*<sup>+/-</sup> mice are partly reflected by alterations in the skeletal muscle insulin signaling pathway. In response to insulin stimulus, the sedentary *Slc2a4*<sup>+/-</sup> mice showed impaired pIR<sup>Y972</sup>, pAkt<sup>T308</sup>, pAkt<sup>S473</sup>, and pAS160<sup>T642</sup> compared to WT mice (Fig. 2A). When *Slc2a4*<sup>+/-</sup> mice were submitted to the endurance exercise training protocol, there was improvement in the pIR<sup>Y972</sup>, pIRS1<sup>Y612</sup>, pAkt<sup>S473</sup>, pAS160<sup>T642</sup>, and pTBC1D1<sup>S237</sup> compared to sedentary *Slc2a4*<sup>+/-</sup> mice (Fig. 2B). In response to the strength exercise training protocol, pIRS1<sup>Y612</sup>, pAkt<sup>T308</sup>, pAkt<sup>S473</sup>, pAS160<sup>T642</sup>, and pTBC1D1<sup>S237</sup> improved compared to sedentary *Slc2a4*<sup>+/-</sup> mice (Fig. 2B). The adaptations from the short-term exercise training protocol were reflected in improved skeletal muscle glucose uptake. The endurance protocol improved basal skeletal muscle glucose uptake. Both protocols restored the impaired insulin-stimulated skeletal muscle glucose uptake in *Slc2a4*<sup>+/-</sup> mice (Fig. 2C, D).

To access possible pathways related to endurance and strength exercise training adaptation in *Slc2a4*<sup>+/-</sup> mice, skeletal muscle (gastrocnemius) samples were collected and submitted to bulk RNA-seq analysis (Fig. 2E). Firstly, distinct genes were down/upregulated by endurance or strength exercise training protocols compared to sedentary *Slc2a4*<sup>+/-</sup> mice (Fig. 2F–I). Regarding the endurance exercise training protocol, 92 genes were upregulated and 81 downregulated compared to sedentary *Slc2a4*<sup>+/-</sup> mice (Fig. 2G). The strength exercise training protocol upregulated 243 genes and downregulated 138 genes compared to sedentary *Slc2a4*<sup>+/-</sup> mice (Fig. 2I). Among these regulated genes, 8 genes (*Cdh4*, *Ctgf1*, *Gas1*, *Hey1*, *Penk*, *Ptprb*, *Amd2*, and *Sorbs2*) were commonly downregulated by endurance and strength exercise training protocols compared to sedentary *Slc2a4*<sup>+/-</sup> mice (Fig. 2J). On the other hand, 17 genes (*Hspb1*, *Hspa1a*, *Hspa1b*, *Hspa9*, *Hspb7*, *Dnaja4*, *Fads6*, *Hadha*, *Ogdha*, *Bcl2l13*, *Retsat*, *Srxn1*, *Irx3*, *Klhl40*, *Lmcd1*, *Ninj1*, and *Nfic*) were upregulated by both exercise training protocols (Fig. 2J). The modulation of these genes was associated with distinct biological

processes, cellular components, and molecular functions, where both endurance and strength exercise protocols showed an association with mitochondrial function (Fig. S2). Moreover, significant transcriptional changes were observed when comparing the strength and endurance exercise protocols in *Slc2a4*<sup>+/-</sup> mice (568 upregulated and 311 downregulated in strength exercise) (Fig. 2L). It is also important to highlight that the effects of exercise observed at the physiological and molecular levels in the *Slc2a4*<sup>+/-</sup> mice were independent of alterations in behavioral responses or corticosterone levels, emphasizing that neither exercise protocol was stressful for the animals (Fig. S3).

### Mitochondrial markers and respiration are impaired in *Slc2a4*<sup>+/-</sup> mice, but endurance training restores them

As gene ontology terms indicated mitochondrial adaptations as important components of the muscle response to PA in *Slc2a4*<sup>+/-</sup> mice, we investigated mitochondrial modulations in the skeletal muscle of *Slc2a4*<sup>+/-</sup> mice, including mitochondrial unfolded protein response markers (UPRmt). Firstly, we observed a lower content of mitochondrial markers (CI-NDUFB8 and Tfam) in the skeletal muscle of *Slc2a4*<sup>+/-</sup> mice compared to WT (Fig. 3A–C). Moreover, this was associated with lower content of UPRmt markers (YME1L1 and CLPP), and a trend ( $p=0.07$ ) to decreased LONP1, which was accompanied by lower mitochondrial respiration (Fig. 3C, D). Importantly, these physiological and molecular alterations were not associated with a compensatory browning effect in the white adipose tissue (pgWAT and ingWAT) and brown adipose tissue, only an augment in *Ucp1* mRNA in the strength group compared to sedentary *Slc2a4*<sup>+/-</sup> mice (Fig. S4).

When *Slc2a4*<sup>+/-</sup> mice performed the endurance or strength exercise training protocol, there were transcriptional changes in OXPHOS-related genes and mitochondrial and UPRmt markers compared to sedentary *Slc2a4*<sup>+/-</sup> mice (Fig. 3E, F). The protein contents of CIII-UQCRC2, CIV-MTCO1, CII-SDHB, Tfam, HSP60, and YME1L1 were upregulated by the endurance exercise protocol compared to sedentary *Slc2a4*<sup>+/-</sup> mice, a fact that was accompanied by increased mitonuclear imbalance and improved mitochondrial respiration in skeletal muscle (Fig. 3G–J). Conversely, the strength exercise training protocol increased CIII-UQCRC2, CIV-MTCO1, Tfam, and OPA1, but did not improve mitochondrial function in the skeletal muscle of *Slc2a4*<sup>+/-</sup> mice (Fig. 3G–J). This result may explain the lower RER found only in the endurance exercised mice (Fig. S5).

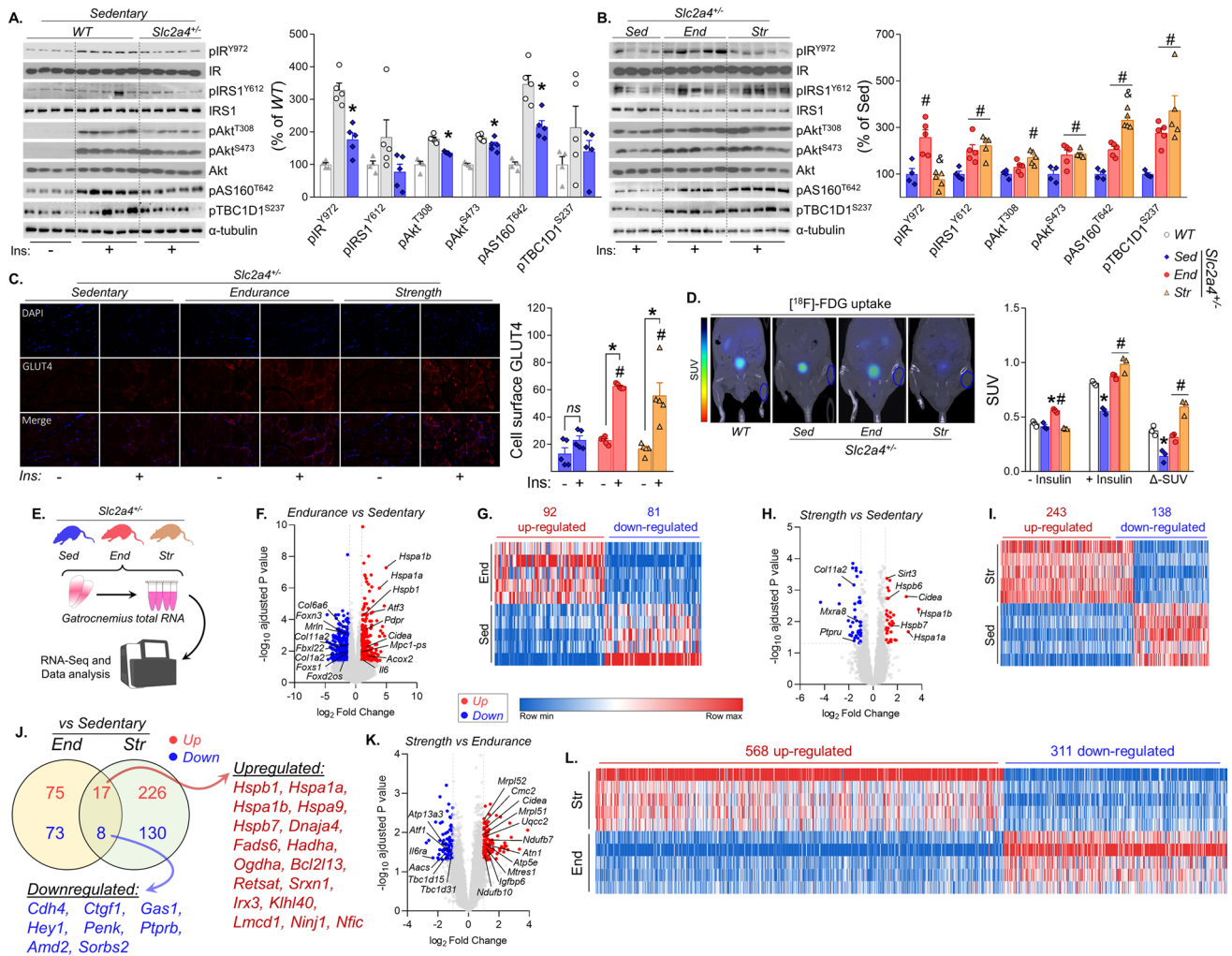


**Fig. 2** Insulin signaling and protein synthesis pathway in skeletal muscle. **A** pIR<sup>Y972</sup>, pIRS1<sup>Y612</sup>, pAkt<sup>T308</sup>, pAkt<sup>S473</sup>, pAS160<sup>T642</sup>, pTBC1D1<sup>S237</sup> protein levels in the skeletal muscle of WT and *Slc2a4*<sup>+/-</sup> mice. **B** Insulin signaling-related protein levels (pIR<sup>Y972</sup>, pIRS1<sup>Y612</sup>, pAkt<sup>T308</sup>, pAkt<sup>S473</sup>, pAS160<sup>T642</sup>, pTBC1D1<sup>S237</sup>) in the skeletal muscle of *Slc2a4*<sup>+/-</sup> and *Slc2a4*<sup>+/-</sup> Endurance and Strength groups. **C** GLUT4 immunofluorescence in the plasma membrane of the gastrocnemius muscle in response to insulin. **D** Standardized uptake value (SUV) of [<sup>18</sup>F]-FDG uptake in the skeletal muscle of WT and *Slc2a4*<sup>+/-</sup> groups. **E** Schematic representation of the samples used in the RNA-seq. **F** Volcano plot of genes differentially expressed between *Slc2a4*<sup>+/-</sup> Endurance vs. *Slc2a4*<sup>+/-</sup> Sedentary group. **G** Heatmap of up/downregulated genes between *Slc2a4*<sup>+/-</sup> Endurance

vs. *Slc2a4*<sup>+/-</sup> Sedentary group. **H** Volcano plot of genes differentially expressed between *Slc2a4*<sup>+/-</sup> Strength vs. *Slc2a4*<sup>+/-</sup> Sedentary group. **I** Heatmap of up/downregulated genes between *Slc2a4*<sup>+/-</sup> Strength vs. *Slc2a4*<sup>+/-</sup> Sedentary group. **J** Venn diagram and common up/down-regulated genes in response to endurance and strength exercise training compared to *Slc2a4*<sup>+/-</sup> Sedentary group. **K** Volcano plot of genes differentially expressed between *Slc2a4*<sup>+/-</sup> Strength vs. *Slc2a4*<sup>+/-</sup> Endurance group. **L** Heatmap of up/downregulated genes between *Slc2a4*<sup>+/-</sup> Strength vs. *Slc2a4*<sup>+/-</sup> Endurance group. In **A**, **B**, n=4, 5, 5 was used. In **C**, n=5/group was used. In **D**, n=3/group was used. \*p<0.05 vs WT group. #p<0.05 vs *Slc2a4*<sup>+/-</sup> Sedentary group. The RNA-seq was performed using gastrocnemius skeletal muscle (n=5/group)

**Fasting glycemia and insulin are correlated with mitochondrial alterations in *Slc2a4*<sup>+/-</sup> mice**

Because our model is hyperglycemic and hyperinsulinemic, we correlated the fasting glucose and insulin levels of the *Slc2a4*<sup>+/-</sup> mice with OXPHOS and UPRmt-related genes in skeletal muscle. In general, most of these genes were negatively correlated with fasting glucose (*Atp5a1*, *Uqc*, *Sdhb*, *Ndufv1*, *Shmt2*, *Lonp1*, *Pink1*) and fasting insulin

(*Atp5a1*, *Uqc*, *Uqcrc1*, *Sdha*, *Sdhb*, *Ndufv1*, *Shmt2*, *Tfam*, *Opa1*, *Vdac*, *Hspd1*, *Lonp1*, *Pink1*) (Fig. 4A, B). Thus, we tested if glucose or insulin could affect mitochondrial markers and function in C2C12 cells (Fig. 4C). The exposure of C2C12 cells to insulin (50 nM, 24 h) decreased CIV-MTCO1, CII-SDHB, and CI-NDUFB8 protein contents, as well as mitonuclear imbalance (Fig. 4D–E). These changes were accompanied by downregulation of *Tfam*, *OPA1*, *VDAC*, and *HSP60*, upregulation of *YME1L1*, a trend to



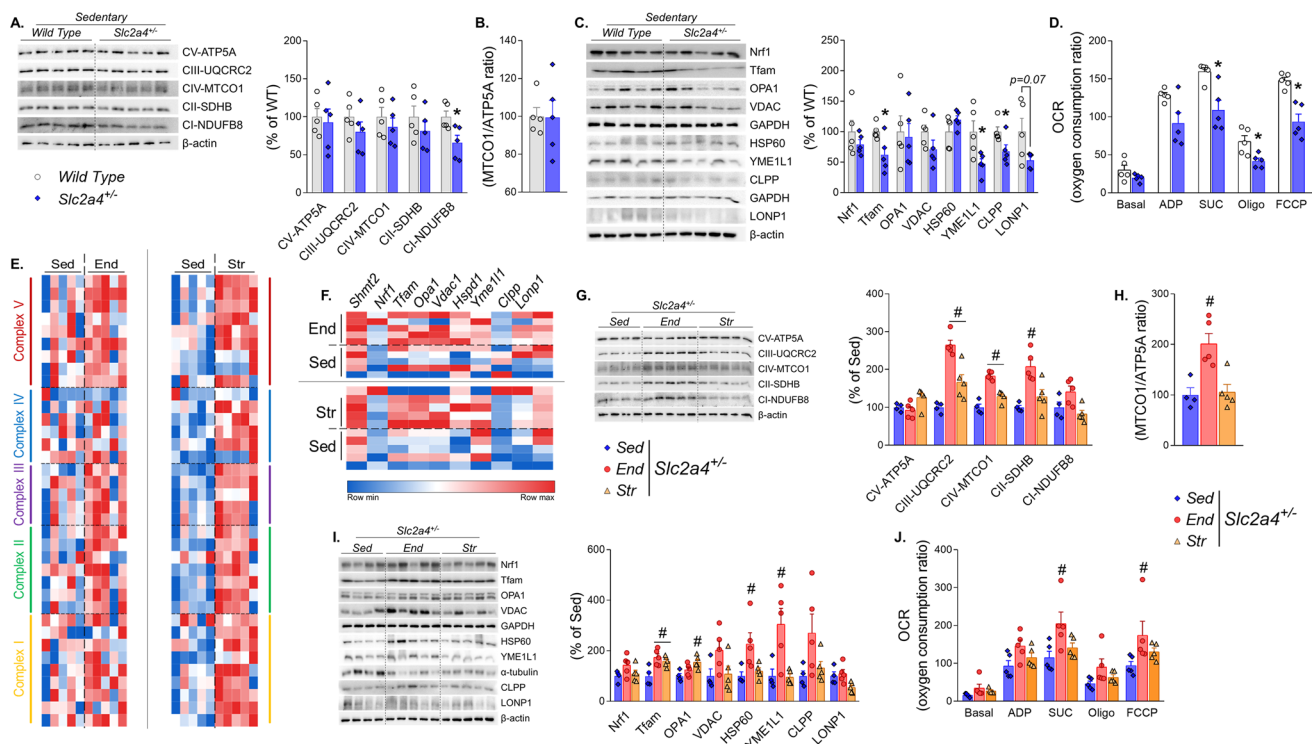


**Fig. 3** Mitochondrial markers and function in the skeletal muscle of *Slc2a4*<sup>+/-</sup> mice. **A** OXPHOS markers (CV-ATP5A, CIII-UQCRC2, CIV-MTCO1, CII-SDHB, and CI-NDUFB8) in the skeletal muscle of WT and *Slc2a4*<sup>+/-</sup> mice. **B** Mitonuclear imbalance (MTCO1/ATP5A) in the skeletal muscle of WT and *Slc2a4*<sup>+/-</sup> mice. **C** Mitochondrial and UPRmt markers (Nrf1, Tfam, OPA1, VDAC, HSP60, YME1L1, CLPP, and LONP1) in the skeletal muscle of WT and *Slc2a4*<sup>+/-</sup> mice. **D** Mitochondrial function in the skeletal muscle of WT and *Slc2a4*<sup>+/-</sup> mice. **E** Heatmap of OXPHOS related genes comparing *Slc2a4*<sup>+/-</sup> Endurance and Strength vs. *Slc2a4*<sup>+/-</sup> Sedentary group. **F** Heatmap of mitochondrial and UPRmt related genes comparing

*Slc2a4*<sup>+/-</sup> Endurance and Strength vs. *Slc2a4*<sup>+/-</sup> Sedentary group. **G** OXPHOS markers (CV-ATP5A, CIII-UQCRC2, CIV-MTCO1, CII-SDHB, and CI-NDUFB8) in the skeletal muscle of sedentary and exercised *Slc2a4*<sup>+/-</sup> mice. **H** Mitonuclear imbalance (MTCO1/ATP5A) in the skeletal muscle of sedentary and exercised *Slc2a4*<sup>+/-</sup> mice. **I** Mitochondrial and UPRmt markers (Nrf1, Tfam, OPA1, VDAC, HSP60, YME1L1, CLPP, and LONP1) in the skeletal muscle of sedentary and exercised *Slc2a4*<sup>+/-</sup> mice. **J** Mitochondrial function in the skeletal muscle of sedentary and exercised *Slc2a4*<sup>+/-</sup> mice. In **A–F**,  $n=5$ /group was used. In **G–J**,  $n=4, 5$  was used. \* $p < 0.05$  vs WT group. # $p < 0.05$  vs *Slc2a4*<sup>+/-</sup> Sedentary group

increased LONP1, and a trend to decreased Nrf1 and CLPP in response to insulin (Fig. 4F). These molecular changes could not modulate the mitochondrial function in C2C12 cells (Fig. 4G). When C2C12 cells were cultured in a low or high glucose medium, there was a decrease in the protein content of CV-ATP5A, CIII-UQCRC2, CII-SDHB, and CI-NDUFB8 and an increase in CIV-MTCO1 in the high glucose group (Fig. 4H, I). In the high glucose group, C2C12 cells showed increased mitonuclear imbalance, Nrf1, and LONP1 content, but lower Tfam, OPA1, VDAC, CLPP, and a trend to decreased HSP60 content, which was associated with a trend to reduced mitochondrial respiration in response to FCCP (Fig. 4K, L).

### Mitochondrial impairments could impact insulin signaling and protein synthesis in C2C12 cells

As we observed important alterations in mitochondrial markers and UPRmt in response to hyperglycemia,

hyperinsulinemia, and endurance exercise training, we investigated if alterations in mitochondria using tetracycline (a blocker of mitochondrial protein synthesis) may impact proteins related to the insulin signaling pathway and glucose uptake in C2C12 cells (Fig. 5A–G). Firstly, the cells treated with tetracycline showed lower levels of CV-ATP5A, CIII-UQCRC2, CIV-MTCO1, OPA1, YME1L1, and PINK1, with a reduction in the mitonuclear imbalance, and a trend to decreased CII-SDHB, Tfam, HSP60, and CLPP compared to CTL cells (Fig. 5B–D). Thereafter, when tetracycline-treated cells were stimulated with insulin, there was impaired pAkt<sup>S473</sup>, pAS160<sup>T642</sup>, and glucose uptake compared to CTL-insulin stimulated cells (Fig. 5F, G). Thus, we can speculate that mitochondrial disarrangements can impair insulin signaling and contribute to insulin resistance.

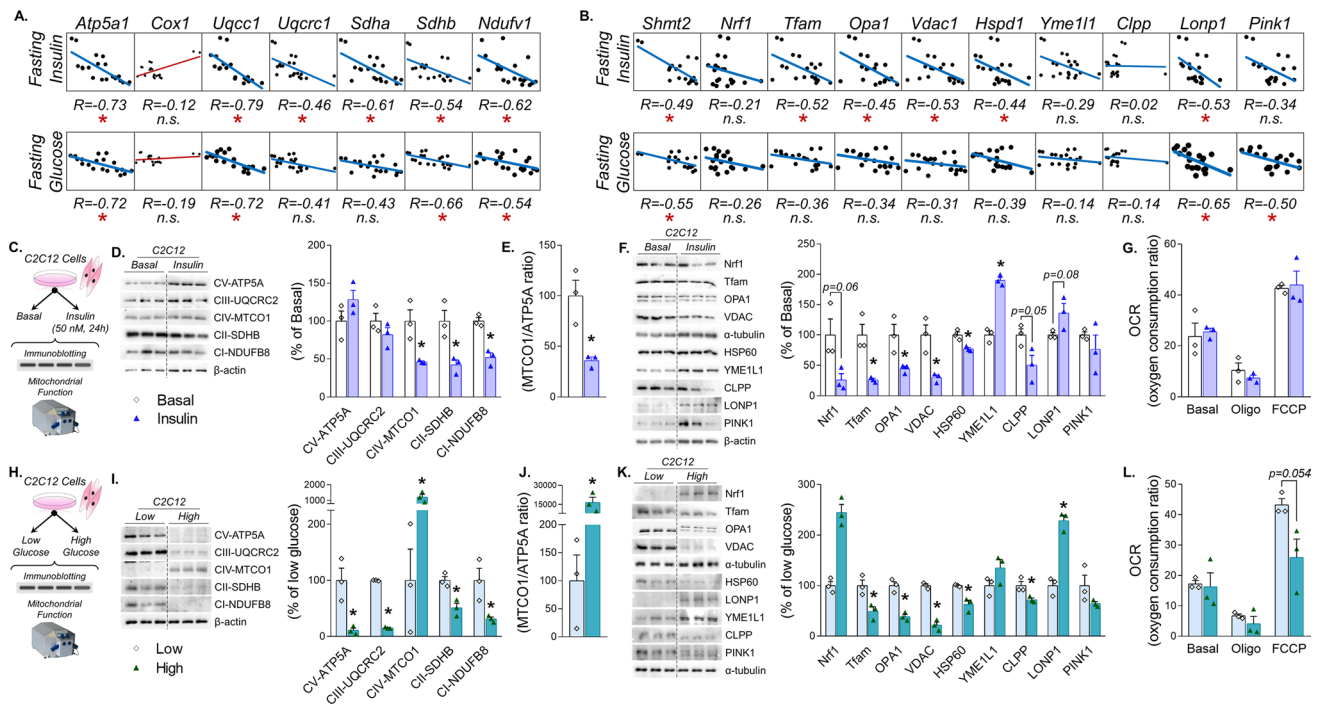


**Fig. 4** Mitochondrial and unfolded protein response markers in skeletal muscle and C2C12 cells. **A** Correlation between fasting insulin or fasting glucose with OXPPOS-related genes. **B** Correlation between fasting insulin or fasting glucose with mitochondrial and UPRmt markers. **C** Schematic figure of insulin treatment in C2C12 cells. **D** OXPPOS markers (CV-ATP5A, CIII-UQCRC2, CIV-MTCO1, CII-SDHB, and CI-NDUF8) in C2C12 cells treated with insulin (50 nM, 24 h). **E** Mitonuclear imbalance (MTCO1/ATP5A). **F** Mitochondrial and UPRmt markers (Nrf1, Tfam, OPA1, VDAC, HSP60, YME1L1, CLPP, and LONP1) in C2C12 cells treated with insulin. **G** Mitochondrial function in C2C12 cells treated with insulin. **H** Sche-

matic figure of low (1000 mg/L)/high glucose (4500 mg/L) treatment in C2C12 cells. **I** OXPPOS markers (CV-ATP5A, CIII-UQCRC2, CIV-MTCO1, CII-SDHB, and CI-NDUF8) in the C2C12 cells treated with low/high glucose. **J** Mitonuclear imbalance (MTCO1/ATP5A). **K** Mitochondrial and UPRmt markers (Nrf1, Tfam, OPA1, VDAC, HSP60, YME1L1, CLPP, and LONP1) in C2C12 cells treated with low/high glucose. **L** Mitochondrial function in C2C12 cells treated with low/high glucose. In **A**, **B**, *R* is the Spearman correlation coefficient between fasting glucose or insulin and the number of genes reads in the RNA-seq. In **D–L**, *n* = 3/group was used. \**p* < 0.05 vs. respective control group (Basal or Low glucose) group

## Strength exercise increases protein synthesis mechanisms in *Slc2a4*<sup>+/-</sup> mice

As muscle adaptations to strength exercise differ from endurance exercise, we evaluated the mechanisms of protein synthesis in *Slc2a4*<sup>+/-</sup> mice submitted to a strength exercise protocol. Detrimental effects in proteins associated with the insulin signaling pathway and protein synthesis (pmTOR<sup>S2448</sup> and pS6K<sup>T389</sup>) were observed in the sedentary *Slc2a4*<sup>+/-</sup> mice (Fig. 6A). In the exhaustion velocity test, both endurance and strength exercised *Slc2a4*<sup>+/-</sup> mice demonstrated improved final velocity compared to the test applied before the exercise training program (Fig. 6B). In the grip strength test and the maximal voluntary carrying capacity (MVCC), the strength exercised *Slc2a4*<sup>+/-</sup> mice, but not the endurance exercised, showed better performance after the exercise training protocol compared to the pre-protocol test (Fig. 6C, D). This was associated with molecular changes in the skeletal muscle, such as increased pS6K<sup>T389</sup> in the endurance exercised mice compared to sedentary

*Slc2a4*<sup>+/-</sup> mice (Fig. 6E). The effects of the strength exercise training protocol were related to increased pIGF1R<sup>Y1131</sup>, pmTOR<sup>S2448</sup>, and pS6K<sup>T389</sup>, accompanied by improved protein synthesis in the skeletal muscle compared to the sedentary group (Fig. 6E and F). In addition, tetracycline-treated cells showed impaired pS6K<sup>T389</sup> and protein synthesis compared to control cells (Fig. 6G and H).

## Discussion

Skeletal muscle is critical to controlling glucose homeostasis, contributing to ~75% of glucose disposal after glucose infusion [5, 6]. Moreover, early defects in skeletal muscle insulin sensitivity are observed in people that develop T2D many years before the disease diagnosis [4]. Identifying early signals before disease establishment could be one key strategy to prevent disease progression. In this scenario, the classical model of insulin resistance [25] as a primary cause of T2D, leading to compensatory hyperinsulinemia

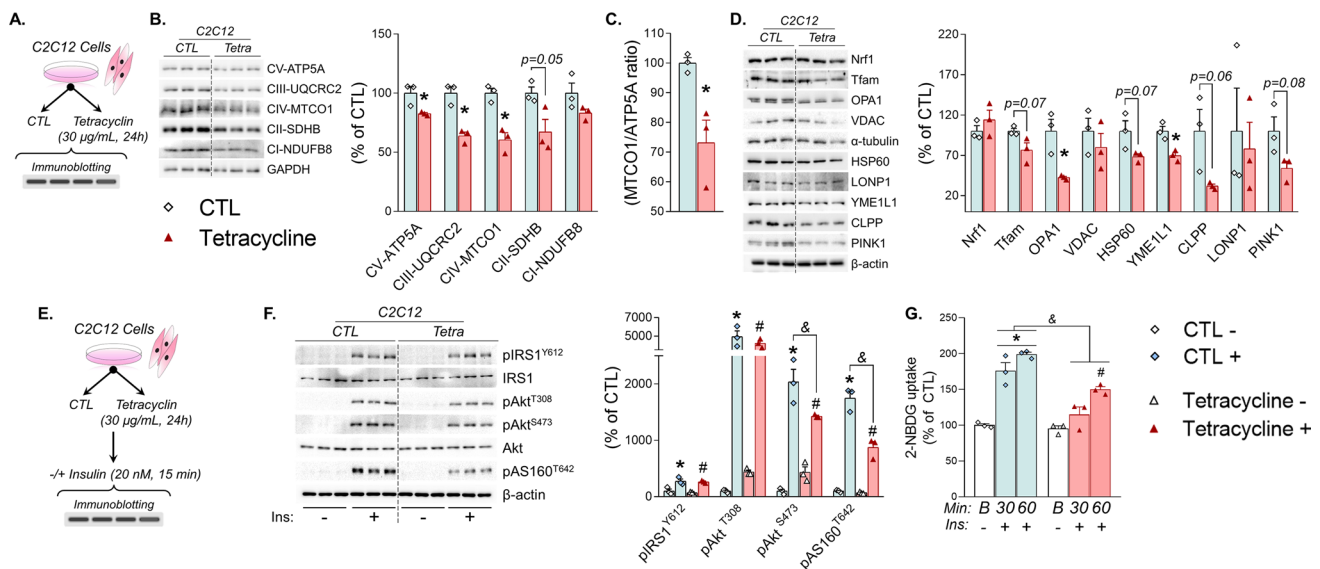


**Fig. 5** Tetracycline induces mitochondrial impairments and insulin signaling defects. **A** Schematic figure of Tetracycline treatment (30 µg/mL, 24 h) in C2C12 cells. **B** OXPHOS markers (CV-ATP5A, CIII-UQCRC2, CIV-MTCO1, CII-SDHB, and CI-NDUFB8) in the tetracycline-treated C2C12 cells. **C** Mitonuclear imbalance (MTCO1/ATP5A). **D** Mitochondrial and UPRmt markers (Nrf1, Tfam, OPA1, VDAC, HSP60, YME1L1, CLPP, and LONP1) in the tetracycline-treated C2C12 cells. **E** Schematic figure of Tetracycline treatment (30 µg/mL, 24 h) followed by insulin stimulus (20 nM, 15 min)

in C2C12 cells. **F** Insulin signaling-related proteins (pIRS1<sup>Y612</sup>, pAkt<sup>T308</sup>, pAkt<sup>S473</sup>, pAS160<sup>T642</sup>) in tetracycline-treated C2C12 cells. **G** 2-NBDG glucose uptake in C2C12 cells in the basal state (**B**), or in response to 30 min of 100 nM insulin (30), or 60 min of 100 nM insulin (60). In **B–G**,  $n=3$ /group was used. In **B–D**,  $*p<0.05$  vs. CTL cells. In graphs **F** and **G**,  $*p<0.05$  vs. CTL(-) or basal cells,  $\#p<0.05$  vs. Tetracycline(-) or basal cells,  $\&p<0.05$  vs. CTL(+)

is controversial in some cases, where hyperinsulinemia is noted before the presence of insulin resistance [26, 27]. Therefore, decreasing insulin circulating levels could be essential to improve metabolic health and prevent metabolic syndrome [9–11]. One possible strategy to control hyperinsulinemia is using physical exercise programs [28, 29], which are regarded as essential to prevent the development of T2D [30].

Modulating insulin levels can cause robust changes in gene networks [31, 32] and post-translational modifications [33, 34]. Likewise, physical exercise is involved in a wide range of gene networks and protein modulations in different tissues to maintain metabolic homeostasis [35]. In this scenario, the investigation of endurance and strength training protocols in animals that are hyperinsulinemic and hyperglycemic under a chow diet may provide new insights into how exercise improves metabolic health. In this study, both short-term endurance and strength exercise training protocols controlled the elevated fasting glucose and insulin, leading to improved whole-body insulin sensitivity and glucose tolerance. This response was accompanied by specific modulations in skeletal muscle at the protein level, where endurance exercise increased pIR<sup>Y972</sup>, pIRS1<sup>Y612</sup>, pAkt<sup>S473</sup>, pAS160<sup>T642</sup>, and pTBC1D1<sup>S237</sup>, while strength exercise increased pIRS1<sup>Y612</sup>, pAkt<sup>T308</sup>, pAkt<sup>S473</sup>, pAS160<sup>T642</sup>, and pTBC1D1<sup>S237</sup> compared to sedentary *Slc2a4*<sup>-/-</sup> mice. These

molecular changes occurred concomitantly with improved skeletal muscle glucose uptake in response to insulin and improved whole-body insulin sensitivity and glucose tolerance. However, the effects of both physical exercise protocols on glycemia and insulinemia were abolished 90 h after the final exercise session. It is worth noting that these findings with respect to the physical exercise protocols were not linked to changes in corticosterone levels and behavioral tests.

To investigate the details of molecular regulation mediated by both short-term exercise training protocols, we performed RNA-seq analysis and protein synthesis assay in the gastrocnemius skeletal muscle of *Slc2a4*<sup>+/-</sup> mice. Strength training promoted robust changes in post-translational mechanisms. After seven days of exercise (and a 16 h wash out), animals subjected to the strength protocol showed increased muscle protein synthesis and strength. This is a very important finding as muscle mass content is directly associated with insulin sensitivity and glucose tolerance [36, 37]. Conversely, results obtained with endurance training are strongly related to transcriptome changes. In addition to the genes explored in this study, the endurance training protocol also increased the *Activating Transcription Factor 3* gene (*Atf3*) and decreased several genes of the forkhead box family (*Foxn3*, *Foxd2os*, *Foxs1*, *Fbxl22*), showing an important action in nuclear

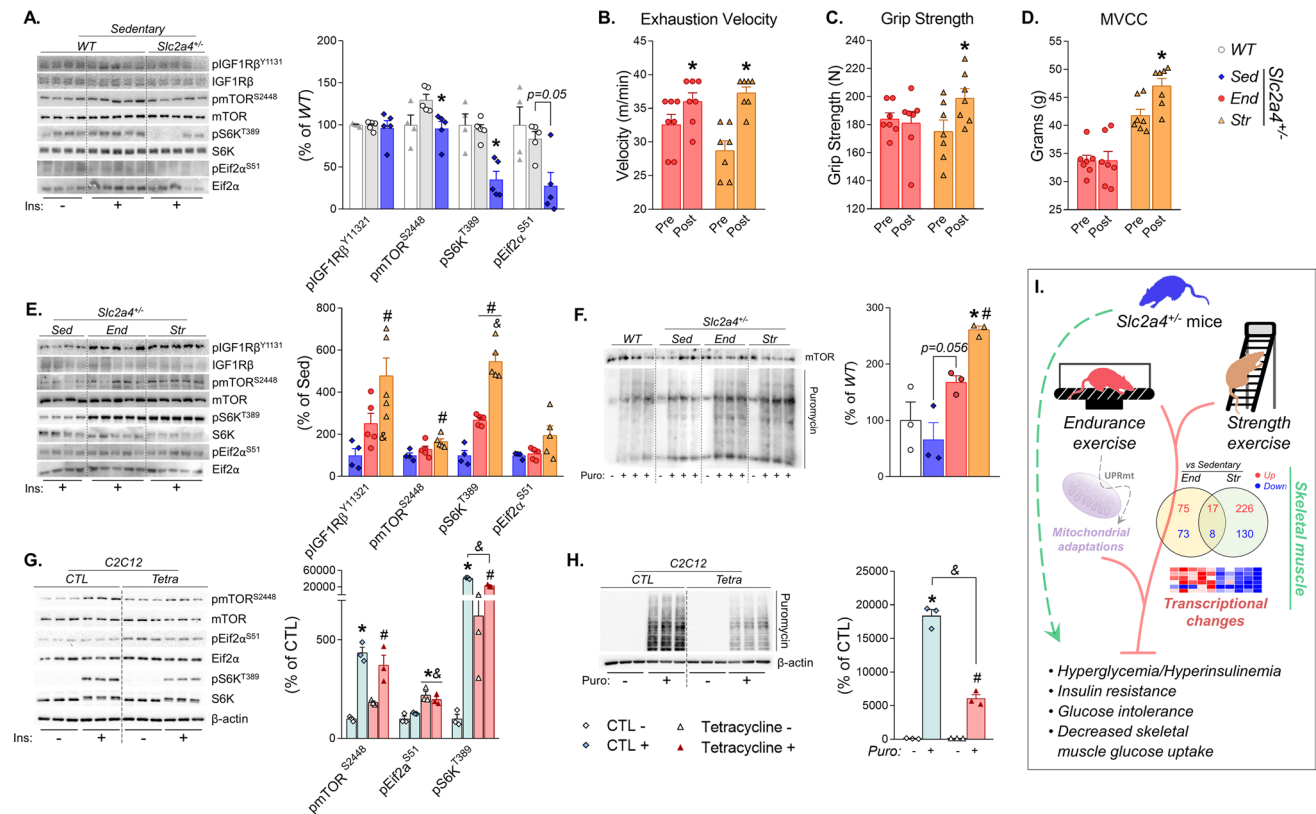


**Fig. 6** Performance tests and protein synthesis in skeletal muscle. **A** Protein synthesis-related proteins (pIGF1Rβ<sup>Y1131</sup>, pmTOR<sup>S2448</sup>, pS6K<sup>T389</sup>, pEIF2α<sup>S51</sup>) in the skeletal muscle of WT and *Slc2a4*<sup>+/-</sup> mice. **B** Exhaustion velocity. **C** Grip strength test. **D** Maximal voluntary carrying capacity (MVCC). **E** Protein synthesis-related proteins (pIGF1Rβ<sup>Y1131</sup>, pmTOR<sup>S2448</sup>, pS6K<sup>T389</sup>, pEIF2α<sup>S51</sup>) in the skeletal muscle of *Slc2a4*<sup>+/-</sup> and *Slc2a4*<sup>+/+</sup> Endurance and Strength groups. **F** Skeletal muscle protein synthesis (anti-Puromycin/mTOR). **G** Protein synthesis-related proteins (pmTOR<sup>S2448</sup>, pEIF2α<sup>S51</sup>, pS6K<sup>T389</sup>) in tetra-

acycline-treated C2C12 cells. **H** Protein synthesis (anti-Puromycin/β-actin) in tetraacycline-treated C2C12 cells. **I** Final schematic figure showing the effects of endurance and strength exercise training on skeletal muscle transcriptome and mitochondrial adaptations in *Slc2a4*<sup>+/-</sup> mice. In **A** and **E**, n = 4, 5, 5/group was used. In **B**, n = 5 was used. In **B**–**D**, n = 7/group was used. In **F**–**H**, n = 3/group was used. In **A**, **E** and **F**, \*p < 0.05 vs WT group. #p < 0.05 vs *Slc2a4*<sup>+/-</sup> Sedentary group. In **G**–**H**, \*p < 0.05 vs. CTL(-) cells, #p < 0.05 vs. Tetraacycline(-) cells, &p < 0.05 vs. CTL(+) cells

transcription factors. The reduction in *Col6a6*, *Col11a2*, and *Colla2* also supports the idea that extracellular matrix modulation participates in the positive effects of physical exercise [38, 39]. Here, we found downregulation of the *Myoregulin* gene (*Mrln*) in the endurance exercised mice, a gene that is negatively correlated with exercise performance [40]. Upregulation of *Il6*, *Acox2*, *Cidea*, *Mpc1-ps*, and *Pdpr* genes in response to endurance training protocol was also found, as well as in several genes related to heat shock proteins (*Hspa1a*, *Hspa1b*, *Hspb1*). In the strength training protocol, we also observed downregulation of genes involved with extracellular matrix (*Coll1a2* and *Mxra8*) and upregulation of heat shock protein-related genes (*Hspa1a*, *Hspa1b*, *Hspb6*, and *Hspb7*). The most significant gene improved by the strength training protocol, *Sirtuin 3* (*Sirt3*), is a well-established deacetylase protein, playing a role in skeletal muscle insulin signaling and mitochondrial fatty acid oxidation [41, 42].

When we compared the transcriptomic signature between strength and endurance training protocols, several genes from the mitochondrial oxidative phosphorylation (OXPHOS) system were upregulated in the strength exercise. However, this modulation was not effective for changing mitochondrial function in the strength exercise group. This may be due to the duration of our protocol, as *PGC-1α4* expression was increased in the skeletal muscle of subjects performing resistance exercise for 3 months [43]. In that study, the authors proposed a mechanism by which resistance exercise increases anaerobic glycolysis and promotes glucose uptake and fatty acid oxidation through *PGC-1α4*, while strength training promotes post-translational mechanisms involved in muscle protein synthesis [43]. The molecular functions related to the upregulated genes observed in both exercise training protocols led us to look at mitochondrial and UPRmt markers in the skeletal muscle of sedentary *Slc2a4*<sup>+/-</sup> mice and C2C12 cells

submitted to different challenges. Evidence suggests that UPRmt may be an essential response to maintaining cellular homeostasis. After mitonuclear imbalance, the UPRmt is an adaptive mechanism to repair and improve mitochondrial function contributing to metabolic health and longevity [44]. This mechanism is well preserved across the species and is sensitive to nutritional and pharmacological interventions [45–47], as well as physical exercise [48–50]. In aged mice presenting mitochondrial defects, four weeks of aerobic treadmill exercise provided the following adaptations in skeletal muscle compared to aged control mice: a increased VDAC; b increased mitochondrial-encoded genes (*mt-ND1*, *mt-CytB*, and *mt-D-loop*); c increased mitonuclear imbalance (MTCO1/ATP5a ratio); and d increased UPRmt makers (HSP60, LONP1, and YME1L1) [49]. In response to high-intensity interval training (4 weeks), aged mice also showed increased mitonuclear imbalance (MTCO1/SDHA ratio) in skeletal muscle compared to aged controls. This result was accompanied by increased *Yme1l1* and *Lonp1* mRNA, as well as increased mitochondrial biogenesis markers (NRF1, Tfam, and VDAC) and mitochondrial-encoded genes (*mt-ND1*, *mt-CytB*, and *mt-D-loop*) [48].

Our data suggest that hyperinsulinemia or hyperglycemia can cause essential alterations in mitochondrial and UPRmt markers at the protein level. The sedentary *Slc2a4<sup>+/-</sup>* mice had lower Tfam, CIII-UQCRC2, YME1L1, and CLPP in skeletal muscle compared to WT, which was associated with lower mitochondrial respiration in response to succinate, oligomycin, and FCCP. The C2C12 cells maintained with high insulin for 24 h demonstrated lower levels of Tfam, VDAC, OPA1, CIII-UQCRC2, CIV-MTCO1, CII-SDHB, CI-NDUFB8, and HSP60, as well as higher levels of YME1L1, compared to basal cells. However, these protein changes were not associated with alterations in mitochondrial function. In addition, maintaining C2C12 in a high glucose medium led to a decrease in Tfam, VDAC, OPA1, CV-ATP5A, CIII-UQCRC2, CII-SDHB, CI-NDUFB8, and CLPP, and an increase in Nrf1, CIV-MTCO1, and LONP1 compared to cells maintained in a low glucose medium. These high glucose cultured cells also demonstrated a trend of lower mitochondrial respiration in response to FCCP.

In skeletal muscle, we observed increased mitochondrial and UPRmt markers (Tfam, VDAC, CV-ATP5A, CIII-UQCRC2, HSP60, and YME1L1) in the endurance exercised *Slc2a4<sup>+/-</sup>* mice compared to sedentary *Slc2a4<sup>+/-</sup>* mice. In contrast, the strength exercise training increased only Tfam and OPA1. This response may explain the improved mitochondrial function observed only in the *Slc2a4<sup>+/-</sup>* mice performing the endurance training protocol. In addition, attenuating mitochondrial markers and UPRmt levels in C2C12 cells led to a reduction in Akt phosphorylation at T308, pAS160, and pS6K. Therefore, alterations in UPRmt may be one of the contributing factors to the changes in

proteins related to skeletal muscle glucose uptake and protein synthesis.

Previous studies have shown the role of doxycycline in the induction of UPRmt with diverse physiological outcomes [44, 51–53]. When *Caenorhabditis Elegans* (*C. Elegans*) were treated with doxycycline, the worms showed lifespan extension, which was associated with lower mitochondrial respiration, mitonuclear imbalance induction, and increased UPRmt [44]. The same authors demonstrated that this mechanism of mitonuclear imbalance and UPRmt induction mediated by doxycycline is preserved in mouse hepatocytes. Moreover, the effects of doxycycline in controlling lifespan in *C. Elegans* are associated with a wide range of gene, protein, and lipid modulations, which are associated with defense response and lipid metabolism [51]. Compared to control mice, long-lived Snell dwarf mice exhibited higher UPRmt in the liver and lower mitochondrial respiration in the primary fibroblasts [53]. This role of doxycycline in longevity stimulation could also be attributed to attenuation in the mitochondrial translation and, consequently, attenuation of cytosolic translation [54]. Therefore, the UPRmt adaptations in the conditions explored in this study could play an important role in the whole-body metabolism.

It is necessary to reinforce that the present study aimed to evaluate the intracellular adaptations in the skeletal muscle linked to metabolism, protein synthesis, and mitochondrial function that occur at the beginning of physical training. Thus, it is known that in this short period, changes in muscle strength from strength training are probably only neuromuscular adaptations. Prolonged strength training increases muscle mass (which does not happen in a short period), which in itself increases glucose disposal. It is likely that resistance training changes do not represent the alterations that would occur in expected mitochondrial remodeling. Therefore, it is probable that some of the results seen here, such as equal increases in response to treadmill running and stair climbing exercises, are not what you would expect from long-term training. In our study, both programs improved skeletal muscle glucose uptake and could suggest feasible strategies to improve metabolic health and prevent type 2 diabetes development (Fig. 6J). Future studies should evaluate other isoforms of glucose transporters in skeletal muscle, such as GLUT1 and GLUT3. This issue was not fully explored in the current investigation and may reveal whether there is any compensation through these Gluts in *Slc2a4<sup>+/-</sup>* mice.

## Conclusion

In summary, the findings of the present study contribute to the prospect of a personalized and targeted prescription in the future of physical exercise. In a complementary and singular way, we expanded the knowledge about the

molecular adaptations occurring at the beginning of aerobic and strength training protocols in a hyperglycemic and hyperinsulinemic GLUT4-deficient mouse model. While endurance exercise plays a vital role in transcriptome and mitochondrial activity, strength exercise mainly affects post-translational mechanisms and protein synthesis. However, both short-term exercise models efficiently improved glycemic homeostasis and overcame the metabolic challenges from *Slc2a4*<sup>+/-</sup> mice. Therefore, performing both types of physical exercise (aerobic and resistance) proved to be a very effective way to mitigate the impacts of hyperglycemia and hyperinsulinemia (metabolic alterations of an insidious and elusive nature) that precede the onset of diabetes.

**Supplementary Information** The online version contains supplementary material available at <https://doi.org/10.1007/s00018-023-04771-2>.

**Author contributions** VRM and JRP wrote the paper and were ultimately responsible for the experiments in this study. VRM, JDB, RCG, ALR, RFLV, SCBRN and GCA. designed and performed the experiments with animals. BMC and RRB performed the mitochondrial function experiments. VRM, MBS, and FMS designed and performed the cell culture experiments. SQB, CDR, and LAV contributed to PET scan experiments. LAV, FMS, LPM, ASRS, ERR, DEC, and JRP contributed to the discussion and laboratory support. All the authors have read, critically revised, and approved this manuscript.

**Funding** This work was supported by FAEPEX, the National Council for Scientific and Technological Development (CNPq; case numbers 303571/2018–7; 140285/2016–4; 442542/2014–3 and 306535/2017–3), the Coordination for the Improvement of Higher Education Personnel (CAPES; finance code 001), and the São Paulo Research Foundation (FAPESP; case numbers 2015/26000–2, 2016/18488–8, 2018/20872–6, 2019/11820–5, 2020/13443–1 and 2021/08692–5).

**Data availability** The data that support the findings of this study are available from the corresponding author upon reasonable request.

## Declarations

**Conflict of interest** The authors of this study have no conflict of interests to declare.

## References

- Wiebe N, Ye F, Crumley ET, Bello A, Stenvinkel P, Tonelli M (2021) Temporal associations among body mass index, fasting insulin, and systemic inflammation. *JAMA Netw Open* 4(3):e211263. <https://doi.org/10.1001/jamanetworkopen.2021.1263>
- Dankner R, Chetrit A, Shanik MHH, Raz I, Roth J (2012) Basal state hyperinsulinemia in healthy normoglycemic adults heralds dysglycemia after more than two decades of follow up. *Diabetes Metab Res Rev* 28(7):618–624. <https://doi.org/10.1002/dmrr.2322>
- Zimmet PZ, Collins VR, Dowse GK, Knight LT (1992) Hyperinsulinaemia in youth is a predictor of type 2 (non-insulin-dependent) diabetes mellitus. *Diabetologia* 35(6):534–541. <https://doi.org/10.1007/BF00400481>
- Rothman DL, Magnusson I, Cline G, Gerard D, Kahn CR, Shulman RG et al (1995) Decreased muscle glucose transport/phosphorylation is an early defect in the pathogenesis of non-insulin-dependent diabetes mellitus. *Proc Natl Acad Sci* 92(4):983–987. <https://doi.org/10.1073/pnas.92.4.983>
- DeFronzo RA, Gunnarsson R, Björkman O, Olsson M, Wahren J (1985) Effects of insulin on peripheral and splanchnic glucose metabolism in noninsulin-dependent (type II) diabetes mellitus. *J Clin Invest* 76(1):149–155. <https://doi.org/10.1172/JCI11938>
- DeFronzo RA, Jacot E, Jequier E, Maeder E, Wahren J, Felber JP (1981) The effect of insulin on the disposal of intravenous glucose: results from indirect calorimetry and hepatic and femoral venous catheterization. *Diabetes* 30(12):1000–1007. <https://doi.org/10.2337/diab.30.12.1000>
- Marangou AG, Weber KM, Boston RC, Aitken PM, Heggie JCP, Kirsner RLG et al (1986) Metabolic consequences of prolonged hyperinsulinemia in humans: evidence for induction of insulin insensitivity. *Diabetes* 35(12):1383–1389. <https://doi.org/10.2337/diab.35.12.1383>
- Cen HH, Hussein B, Botezelli JD, Wang S, Zhang JA, Noursadeghi N et al (2022) Human and mouse muscle transcriptomic analyses identify insulin receptor mRNA downregulation in hyperinsulinemia-associated insulin resistance. *FASEB J*. <https://doi.org/10.1096/fj.202100497RR>
- Page MM, Skovs S, Cen H, Chiu AP, Dionne DA, Hutchinson DF et al (2018) Reducing insulin via conditional partial gene ablation in adults reverses diet-induced weight gain. *FASEB J* 32(3):1196–1206. <https://doi.org/10.1096/fj.201700518R>
- Templeman NM, Flibotte S, Chik JHL, Sinha S, Lim GE, Foster LJ et al (2017) Reduced circulating insulin enhances insulin sensitivity in old mice and extends lifespan. *Cell Rep* 20(2):451–463. <https://doi.org/10.1016/j.celrep.2017.06.048>
- Mehran AE, Templeman NM, Brigidi GS, Lim GE, Chu K-Y, Hu X et al (2012) Hyperinsulinemia drives diet-induced obesity independently of brain insulin production. *Cell Metab* 16(6):723–737. <https://doi.org/10.1016/j.cmet.2012.10.019>
- Huang S, Czech MP (2007) The GLUT4 glucose transporter. *Cell Metab* 5(4):237–252. <https://doi.org/10.1016/j.cmet.2007.03.006>
- Reno CM, Puente EC, Sheng Z, Daphna-Iken D, Bree AJ, Routh VH et al (2017) Brain GLUT4 knockout mice have impaired glucose tolerance, decreased insulin sensitivity, and impaired hypoglycemic counterregulation. *Diabetes* 66(3):587–597. <https://doi.org/10.2337/db16-0917>
- Sylow L, Kleinert M, Richter EA, Jensen TE (2017) Exercise-stimulated glucose uptake—regulation and implications for glycaemic control. *Nat Rev Endocrinol* 13(3):133–148. <https://doi.org/10.1038/nrendo.2016.162>
- Sangwung P, Petersen KF, Shulman GI, Knowles JW (2020) Mitochondrial dysfunction, insulin resistance, and potential genetic implications. *Endocrinology*. <https://doi.org/10.1210/endo/bqaa017>
- Mogensen M, Sahlin K, Fernström M, Glinborg D, Vind BF, Beck-Nielsen H et al (2007) Mitochondrial respiration is decreased in skeletal muscle of patients with type 2 diabetes. *Diabetes* 56(6):1592–1599. <https://doi.org/10.2337/db06-0981>
- Stenbit AE, Tsao TS, Li J, Burcelin R, Geenen DL, Factor SM et al (1997) GLUT4 heterozygous knockout mice develop muscle insulin resistance and diabetes. *Nat Med* 3(10):1096–1101
- Hoene M, Kappler L, Kollipara L, Hu C, Irmeler M, Bleher D et al (2021) Exercise prevents fatty liver by modifying the compensatory response of mitochondrial metabolism to excess substrate availability. *Mol Metab* 54:101359. <https://doi.org/10.1016/j.molmet.2021.101359>
- Fredrickson G, Barrow F, Dietsche K, Parthiban P, Khan S, Robert S et al (2021) Exercise of high intensity ameliorates hepatic inflammation and the progression of NASH. *Mol Metab*. <https://doi.org/10.1016/j.molmet.2021.101270>


20. Macfarlane DP, Forbes S, Walker BR (2008) Glucocorticoids and fatty acid metabolism in humans: fuelling fat redistribution in the metabolic syndrome. *J Endocrinol* 197(2):189–204. <https://doi.org/10.1677/JOE-08-0054>
21. Hawley JAA, Hargreaves M, Joyner MJ, Zierath JRR (2014) Integrative biology of exercise. *Cell* 159(4):738–749. <https://doi.org/10.1016/j.cell.2014.10.029>
22. Komada M, Takao K, Miyakawa T (2008) Elevated Plus Maze for Mice. *J Vis Exp*. <https://doi.org/10.3791/1088>
23. Oliveira de Almeida WA, Maculano Esteves A, Leite de Almeida-Júnior C, Lee KS, Kannebley Frank M, Oliveira Mariano M et al (2014) The effects of long-term dopaminergic treatment on locomotor behavior in rats. *Sleep Sci* 7(4):203–208. <https://doi.org/10.1016/j.sisci.2014.10.003>
24. Bala M, Gupta P, Gupta S, Dua A, Injeti E, Mittal A (2021) Efficient and modified 2-NBDG assay to measure glucose uptake in cultured myotubes. *J Pharmacol Toxicol Methods*. <https://doi.org/10.1016/j.vascn.2021.107069>
25. Roden M, Shulman GI (2019) The integrative biology of type 2 diabetes. *Nature* 576(7785):51–60. <https://doi.org/10.1038/s41586-019-1797-8>
26. Shanik MH, Xu Y, Skrha J, Dankner R, Zick Y, Roth J (2008) Insulin resistance and hyperinsulinemia: is hyperinsulinemia the cart or the horse? *Diabetes Care*. <https://doi.org/10.2337/dc08-s264>
27. Corkey BE (2012) Banting lecture 2011: hyperinsulinemia: cause or consequence? *Diabetes* 61(1):4–13. <https://doi.org/10.2337/db11-1483>
28. Bird SR, Hawley JA (2017) Update on the effects of physical activity on insulin sensitivity in humans. *BMJ Open Sport Exerc Med* 2(1):e000143. <https://doi.org/10.1136/bmjsem-2016-000143>
29. Richter EA, Sylow L, Hargreaves M (2021) Interactions between insulin and exercise. *Biochem J* 478(21):3827–3846. <https://doi.org/10.1042/BCJ20210185>
30. Hu G, Rico-Sanz J, Lakka TA, Tuomilehto J (2006) Exercise, genetics and prevention of type 2 diabetes. *Essays Biochem* 42:177–192. <https://doi.org/10.1042/bse0420177>
31. Rome S, Clément K, Rabasa-Lhoret R, Loizon E, Poitou C, Barsh GS et al (2003) Microarray profiling of human skeletal muscle reveals that insulin regulates ~800 genes during a hyperinsulinemic clamp. *J Biol Chem* 278(20):18063–18068. <https://doi.org/10.1074/jbc.M300293200>
32. Batista TM, Garcia-Martin R, Cai W, Konishi M, O'Neill BT, Sakaguchi M et al (2019) Multi-dimensional transcriptional remodeling by physiological insulin in vivo. *Cell Rep* 26(12):3429–3443. <https://doi.org/10.1016/j.celrep.2019.02.081> (e3)
33. Wolfrum C, Besser D, Luca E, Stoffel M (2003) Insulin regulates the activity of forkhead transcription factor Hnf-3 $\beta$ /Foxa-2 by Akt-mediated phosphorylation and nuclear/cytosolic localization. *Proc Natl Acad Sci* 100(20):11624–11629. <https://doi.org/10.1073/pnas.1931483100>
34. Batista TM, Jayavelu AK, Wewer Albrechtsen NJ, Iovino S, Lebastchi J, Pan H et al (2020) A cell-autonomous signature of dysregulated protein phosphorylation underlies muscle insulin resistance in type 2 diabetes. *Cell Metab* 32(5):844–859. <https://doi.org/10.1016/j.cmet.2020.08.007> (e5)
35. Sato S, Dyar KA, Treebak JT, Jepsen SL, Ehrlich AM, Ashcroft SP et al (2022) Atlas of exercise metabolism reveals time-dependent signatures of metabolic homeostasis. *Cell Metab* 34(2):329–345.e8. <https://doi.org/10.1016/j.cmet.2021.12.016> (e8)
36. Srikanthan P, Karlamangla AS (2011) Relative muscle mass is inversely associated with insulin resistance and prediabetes: findings from the third national health and nutrition examination survey. *J Clin Endocrinol Metab* 96(9):2898–2903. <https://doi.org/10.1210/jc.2011-0435>
37. Kim K, Park SM (2018) Association of muscle mass and fat mass with insulin resistance and the prevalence of metabolic syndrome in Korean adults: a cross-sectional study. *Sci Rep* 8(1):2703. <https://doi.org/10.1038/s41598-018-21168-5>
38. MacDonald TL, Pattamapranont P, Cooney EM, Nava RC, Mitri J, Hafida S et al (2022) Canagliflozin prevents hyperglycemia-associated muscle extracellular matrix accumulation and improves the adaptive response to aerobic exercise. *Diabetes* 71(5):881–893. <https://doi.org/10.2337/db21-0934>
39. MacDonald TL, Pattamapranont P, Pathak P, Fernandez N, Freitas EC, Hafida S et al (2020) Hyperglycaemia is associated with impaired muscle signalling and aerobic adaptation to exercise. *Nat Metab* 2(9):902–917. <https://doi.org/10.1038/s42255-020-0240-7>
40. Anderson DM, Anderson KM, Chang C-L, Makarewicz CA, Nelson BR, McAnally JR et al (2015) A micropeptide encoded by a putative long noncoding rna regulates muscle performance. *Cell* 160(4):595–606. <https://doi.org/10.1016/j.cell.2015.01.009>
41. Hirschey MD, Shimazu T, Goetzman E, Jing E, Schwer B, Lombard DB et al (2010) SIRT3 regulates mitochondrial fatty-acid oxidation by reversible enzyme deacetylation. *Nature* 464(7285):121–125. <https://doi.org/10.1038/nature08778>
42. Jing E, O'Neill BT, Rardin MJ, Kleinridders A, Ilkeyeva OR, Ussar S et al (2013) Sirt3 regulates metabolic flexibility of skeletal muscle through reversible enzymatic deacetylation. *Diabetes* 62(10):3404–3417. <https://doi.org/10.2337/db12-1650>
43. Koh J-H, Pataky MW, Dasari S, Klaus KA, Vuckovic I, Rueggsegger GN et al (2022) Enhancement of anaerobic glycolysis—a role of PGC-1 $\alpha$  in resistance exercise. *Nat Commun* 13(1):2324. <https://doi.org/10.1038/s41467-022-30056-6>
44. Houtkooper RH, Mouchiroud L, Ryu D, Moullan N, Katsyuba E, Knott G et al (2013) Mitonuclear protein imbalance as a conserved longevity mechanism. *Nature* 497(7450):451–457. <https://doi.org/10.1038/nature12188>
45. Zhang H, Ryu D, Wu Y, Gariani K, Wang X, Luan P et al (2016) NAD<sup>+</sup> repletion improves mitochondrial and stem cell function and enhances life span in mice. *Science* 352(6292):1436–1443. <https://doi.org/10.1126/science.aaf2693>
46. Pirinen E, Cantó C, Jo YS, Morato L, Zhang H, Menzies KJ et al (2014) Pharmacological inhibition of poly(ADP-Ribose) polymerases improves fitness and mitochondrial function in skeletal muscle. *Cell Metab* 19(6):1034–1041. <https://doi.org/10.1016/j.cmet.2014.04.002>
47. van de Weijer T, Phielix E, Bilet L, Williams EG, Ropelle ER, Bierwagen A et al (2015) Evidence for a direct effect of the NAD<sup>+</sup> precursor acipimox on muscle mitochondrial function in humans. *Diabetes* 64(4):1193–1201. <https://doi.org/10.2337/db14-0667>
48. Cordeiro AV, Peruca GF, Braga RR, Bricola RS, Lenhare L, Silva VRR et al (2021) High-intensity exercise training induces mitonuclear imbalance and activates the mitochondrial unfolded protein response in the skeletal muscle of aged mice. *GeroScience* 43(3):1513–1518. <https://doi.org/10.1007/s11357-020-00246-5>
49. Cordeiro AV, Bricola RS, Braga RR, Lenhare L, Silva VRR, Anaruma CP et al (2020) Aerobic Exercise Training Induces the Mitonuclear Imbalance and UPRmt in the Skeletal Muscle of Aged Mice. *J Gerontol Series A* 75(12):2258–2261. <https://doi.org/10.1093/gerona/glaa059>
50. Braga RR, Crisol BM, Bricola RS, Sant'ana MR, Nakandakari SCBR, Costa SO et al (2021) Exercise alters the mitochondrial proteostasis and induces the mitonuclear imbalance and UPRmt in the hypothalamus of mice. *Sci Rep*. <https://doi.org/10.1038/s41598-021-82352-8>
51. Gao AW, El Alam G, Lalou A, Li TY, Molenaars M, Zhu Y et al (2022) Multi-omics analysis identifies essential regulators of mitochondrial stress response in two wild-type *C. elegans* strains. *IScience* 25(2):103734. <https://doi.org/10.1016/j.isci.2022.103734>

52. Moullan N, Mouchiroud L, Wang X, Ryu D, Williams EG, Mottis A et al (2015) Tetracyclines disturb mitochondrial function across eukaryotic models: a call for caution in biomedical research. *Cell Rep* 10(10):1681–1691. <https://doi.org/10.1016/j.celrep.2015.02.034>
53. Ozkurede U, Miller RA (2019) Improved mitochondrial stress response in long-lived Snell dwarf mice. *Aging Cell*. <https://doi.org/10.1111/ace1.13030>
54. Molenaars M, Janssens GE, Williams EG, Jongejan A, Lan J, Rabot S et al (2020) A conserved mito-cytosolic translational balance links two longevity pathways. *Cell Metab* 31(3):549–563. <https://doi.org/10.1016/j.cmet.2020.01.011> (e7)

**Publisher's Note** Springer Nature remains neutral with regard to jurisdictional claims in published maps and institutional affiliations.

Springer Nature or its licensor (e.g. a society or other partner) holds exclusive rights to this article under a publishing agreement with the author(s) or other rightsholder(s); author self-archiving of the accepted manuscript version of this article is solely governed by the terms of such publishing agreement and applicable law.

## Authors and Affiliations

Vitor Rosetto Muñoz<sup>1</sup>  · José Diego Botezelli<sup>1</sup> · Rafael Calais Gaspar<sup>1</sup> · Alisson L. da Rocha<sup>1</sup> · Renan Fudoli Lins Vieira<sup>1</sup> · Barbara Moreira Crisol<sup>1</sup> · Renata Rosseto Braga<sup>1</sup> · Matheus Brandemarte Severino<sup>2</sup> · Susana Castelo Branco Ramos Nakandakari<sup>3</sup> · Gabriel Calheiros Antunes<sup>1</sup> · Sérgio Q. Brunetto<sup>4</sup> · Celso D. Ramos<sup>4,5</sup> · Lício Augusto Velloso<sup>6,7</sup> · Fernando Moreira Simabuco<sup>2</sup> · Leandro Pereira de Moura<sup>1,6</sup> · Adelino Sanchez Ramos da Silva<sup>8</sup> · Eduardo Rochete Ropelle<sup>1,6,9</sup> · Dennys Esper Cintra<sup>3,6</sup> · José Rodrigo Pauli<sup>1,6,9</sup>

José Diego Botezelli  
jdbotezelli@gmail.com

<sup>1</sup> Laboratory of Molecular Biology of Exercise, University of Campinas (UNICAMP), Limeira, São Paulo, Brazil

<sup>2</sup> Multidisciplinary Laboratory of Food and Health (LabMAS), School of Applied Sciences (FCA), University of Campinas (UNICAMP), Limeira, São Paulo, Brazil

<sup>3</sup> Laboratory of Nutritional Genomics, University of Campinas (UNICAMP), Limeira,, São Paulo, Brazil

<sup>4</sup> Biomedical Engineering Center, University of Campinas (UNICAMP), Campinas, São Paulo, Brazil

<sup>5</sup> Department of Radiology, University of Campinas, Campinas, São Paulo 13084-970, Brazil

<sup>6</sup> OCRC - Obesity and Comorbidities Research Center, University of Campinas (UNICAMP), Campinas, São Paulo, Brazil

<sup>7</sup> Laboratory of Cell Signaling, Department of Internal Medicine, University of Campinas, Campinas, São Paulo 13084-970, Brazil

<sup>8</sup> Postgraduate Program in Rehabilitation and Functional Performance, Ribeirão, Preto Medical School, University of São Paulo (USP), School of Physical Education and Sport of Ribeirão Preto, Ribeirão Preto, São Paulo, Brazil

<sup>9</sup> National Institute of Science and Technology of Obesity and Diabetes, University of Campinas (UNICAMP), Campinas, São Paulo, Brazil